FATIGUE FRACTURE OF LOW ALLOY STEEL AT ULTRA-HIGH-CYCLE REGION UNDER ELEVATED TEMPERATURE CONDITION

K.Kanazawa* and S.Nishijima †

Elevated temperature, high-cycle fatigue behaviors of low alloy steel were discussed from viewpoint of effect of oxidation on fracture mechanism. Stepwise S-N curves were obtained for fatigue data tested at 300 and 400℃. Surface fracture and internal fracture with fish-eye pattern were dominant under high stress and low stress levels, respectively. Under the latter condition, surface fracture did not occur because of oxidation effect, nevertheless, fish-eye fracture occurred by initiation and propagation processes of internal crack. Fatigue behavior under internal fracture should be called ultra-high-cycle fatigue and be discussed in distinction from fatigue behavior under surface fracture what is called high-cycle fatigue as usual.

INTRODUCTION

For conventional carbon and low alloy steels, fatigue fracture occurred under initiation and propagation processes of surface crack and fatigue limits were recognized in fatigue data tested up to 10^7 cycles at room temperature. Internal fractures, where fish-eye pattern was observed on fatigue fracture surfaces, occurred frequently for high strength steels (1) and surface treated steels such as induction hardened (2) or carburized steels (3). Fish-eye pattern was also observed for conventional steels on a fracture surface fatigued at elevated temperatures and at cycles above about 10^7 (4). The reason why fish-eye fatigue fracture occurs at elevated temperature and whether fatigue limit for internal fracture exits or not have not been clarified.

In this paper, fatigue behavior of high-cycle region up to 10^9 cycles at elevated temperatures was discussed for low alloy steel JIS SCMV 2 from viewpoints of effect of oxidation on fracture mechanism by using data published previously (5) and some additional data.

* Department of Precision Mechanics, Chuo University.
† Kawasaki Heavy Industries, Ltd.

EXPERIMENTAL

The material examined was an normalized-tempered 1Cr-0.5Mo steel plate specified in JIS as SCMV 2 which consists of ferritic and pearlitic structures. Fatigue tests were carried out up to 10^8 cycles under a frequency of 100Hz at temperatures from room temperature to 400℃ using 4-points rotating bending fatigue testing machines with an electric furnace. The fatigue test specimen used had a parallel part 8mm in diameter. Numerical fatigue data themselves were published in NRIM Fatigue Data Sheet (5).

RESULTS AND DISCUSSION

Figure 1 shows fatigue S-N curves for various test temperatures. Conventional S-N curves were obtained at room temperature and 200℃. On the other hand, stepwise S-N curves were recognized for fatigue data tested at 300 and 400℃. Fatigue cracks initiated at surface and at interior of the specimens under high stress and low stress levels, respectively, of the stepwise S-N curve. When crack initiated at interior of the specimen, fish-eye pattern was observed at the fracture surface, which example is shown in Figure 2. The stepwise S-N curve is caused by the difference in crack initiation site.

Phenomenon of the stepwise S-N curve is of great interest. It is very important to confirm whether fatigue limit exists or not under the condition of internal fracture with fish-eye pattern. Additional fatigue tests were carried out at 300 and 400℃ under lower stress levels than the fatigue strength at 10^8 cycles. According to the results plotted in Figure 1, fatigue limit was not recognized at 400℃ by tests up to 10^9 cycles.

In induction hardened or carburized steels, residual compressive stress at the surface layer plays an important role for surface fracture not to occur and then fish-eye fracture occurs by initiation and propagation processes of internal crack. In the present material, surface fracture did not occur at high cycle region tested at 300 and 400℃. Why? Surface of the specimen was oxidized during the fatigue test at high temperatures. It is considered as one reason that crack propagation process is delayed by crack closure due to oxide (6). But any non-propagating surface crack was not recognized at cross section of the fatigued specimen with fish-eye pattern in spite of careful observation. Hardness of oxidized surface layer was higher than hardness of the matrix. A surface crack is hard to initiate at elevated temperatures under low stress levels, as the oxidized surface layer prevents dislocation from exiting through the surface. During this period, a crack initiates and propagates from an internal defect such as non-metallic inclusions, and then fish-eye fracture occurs.

It is well known that there is a good correlation between the fatigue strength and tensile strength for conventional steels at room temperature (7). But, this relationship does not apply to results obtained for carbon and low alloy steels at intermediate temperatures at which dynamic strain aging occurs. Fatigue strength at this temperature range is higher than that estimated from tensile strength.

Figure 3 shows temperature dependencies of deformation and strength properties such as 0.2% proof stress σ_y, cyclic proof stress σ_{yc}, tensile strength σ_B and fatigue strength at 10^8 cycles σ_{wb}. Where, cyclic proof stress means 0.2% proof stress in a cyclic stress-strain curve obtained by incremental step method. The ordinate of Figure 3 means the non-dimensional values κ which are deformation and strength properties divided by their values at room temperature. The subscripts for κ mean the same as those for σ.

In view of temperature dependency of dislocation movement, the curves of κ_y, κ_B and κ_{yc} may show the same tendency as each other. But the curves of κ_B and κ_{yc} are located at higher levels than that of κ_y at temperature region of 300 and 400℃. Hardening due to dynamic strain aging is concerned in these behaviors. As for curves of κ_B and κ_{yc}, the latter is located at higher level than the former. This means that hardening due to dynamic strain aging under cyclic tensile and compressive straining is more remarkable than that under monotonic tensile straining.

In Figure 3, temperature dependence of κ_{wb} is not similar to the tendency of κ_B, but to the tendency of κ_{yc}. Increasing of fatigue strength of carbon and low alloy steels at intermediate temperatures is caused by strengthening of matrix by dynamic strain aging. Evaluation of the effect of dynamic strain aging on fatigue strength should be done by cyclic proof stress, as dynamic strain aging under cyclic straining is reflected to cyclic proof stress.

Figure 4 shows σ_a/σ_{yc}-N_f curves which ordinate is stress amplitude normalized by cyclic proof stress of test temperature. σ_a/σ_{yc}-N_f curves are classified into two groups independently of test temperatures. One is for surface fracture at relatively low-cycle region and the other is for internal fracture with fish-eye pattern at relatively high-cycle region. Transition level of σ_a/σ_{yc} from surface fracture to internal fracture depends on temperature condition. The lowest level is for results of room temperature and 200℃, and the highest one is for result of 400℃. As a reason of this phenomenon, it is considered that the higher the test temperature, the more rapidly oxidized layer, which prevents surface crack from initiating, is formed at the specimen surface.

Figure 4 shows that internal fracture occurs at lower levels of σ_a/σ_{yc} than that corresponding to fatigue limits at room temperature and 200℃. This phenomenon reflects the essential difference between fracture modes of surface crack and internal crack. That is, crack propagation process of surface crack is affected strongly by oxidation, nevertheless crack propagation process of internal crack is scarcely affected by oxidation. Propagation of an internal crack proceeds under vacuum condition. Threshold level of propagation for Mode I crack under vacuum condition is lower than that under conditions of oxidization or absorption as pointed out by Meyn(8). Fatigue limit relating to internal crack may be lower than fatigue limit relating to surface crack. It is considered that the lowest value of fatigue limit for internal fracture is dominated by the emission limit of dislocation at crack tip (9). This result suggests an important phenomenon. That is, fatigue fracture by internal crack may occur at cycles above 10^8 under lower stress levels than fatigue strength at 10^8 cycles at room temperature and 200℃.

Fatigue behavior which has been called high-cycle fatigue can be classified clearly into two groups: surface fracture dominant and internal fracture dominant. Fatigue behavior under internal fracture dominant should be called ultra-high-cycle fatigue and should be discussed in distinction from fatigue behavior under surface fracture dominant which is called high-cycle fatigue as usual.

CONCLUSION

Elevated temperature, high-cycle fatigue behavior of low alloy steel SCMV 2 were discussed from viewpoint of effect of oxidation on fracture mechanism. The results obtained are as follows:

(1) Stepwise S-N curves were obtained for fatigue data tested at 300 and 400℃. Surface fracture and internal fracture with fish-eye pattern were dominant at relatively low-cycle and high-cycle regions, respectively.

(2) Fatigue limits was not recognized by tests up to 10^9 cycles at 400℃.

(3) At high cycle region tested at 300 and 400℃, surface fracture did not occur because of oxidation effect: nevertheless, fish-eye fracture occurred by initiation and propagation processes of internal crack.

(4) Temperature dependency of fatigue strength due to dynamic strain aging was not estimated by tensile strength but by cyclic proof stress.

(5) σ_a/σ_{yc}-N_f curves were classified into two groups independently of test temperature: groups of surface fracture dominant and internal fracture dominant such as fish-eye pattern.

(6) Fatigue behavior under internal fracture should be called ultra-high-cycle fatigue and be discussed in distinction from fatigue behavior under surface fracture what is called high-cycle fatigue.

REFERENCES

(1) Kawada, Y., Nakazawa, H. and Kodama, S., Trans. Japan Soc. Mech. Eng., Vol. 29 I., 1963, pp.1674-1683.

(2) Kimura, K., Yamada, K., Simizu, M. and Kunio, T., Trans. Japan Soc. Mech. Eng., Vol. 35 I., 1969, pp.2146-2153.

(3) Masuda, C., Nishijima, S. and Shimodaira, M., Trans. Japan Soc. Mech. Eng., Vol. 49A., 1983, pp.413-423.

(4) Kanazawa, K., Sato, M., Kimura, M. and Nishijima, S., J. of Soc. Mat. Sci. Japan, Vol.37., 1988, pp.1423-1428.

(5) "NRIM Fatigue Data Sheet", No.72., National Research Institute for Metals, Japan, 1992.

(6) Haigh, J. R., Eng. Fract. Mech., Vol7., 1975, pp.271-284.

(7) Nishijima, S., Ishii, A., Kanazawa, K., Masuda, C. and Matsuoka, S., "NRIM Fatigue Data Sheet Technical Document", No.5, National Research Institute for Metals, Japan, 1989.

(8) Meyn, D. A., Trans. ASM, Vol. 61.,1968, pp52-61.

(9) Yokobori, A. T. and Yokobori, T., "Fatigue Threshold", Vol. 2., 1982, pp.171-189, EMAS Ltd.

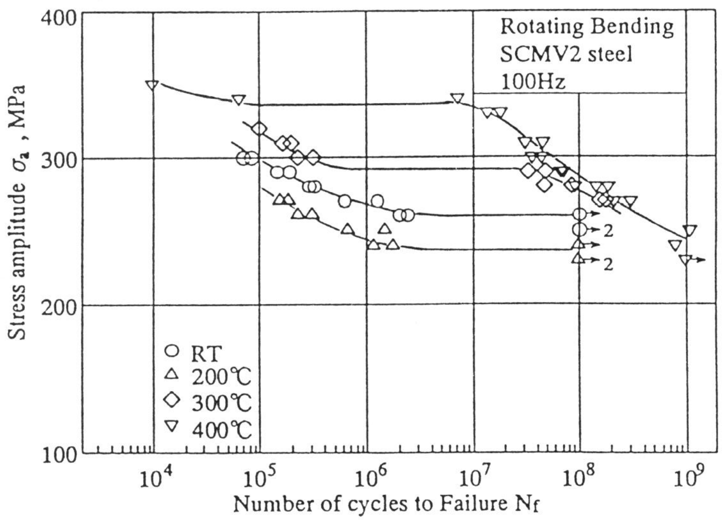

Figure 1 Rotating bending fatigue S-N curves obtained at various test temperatures

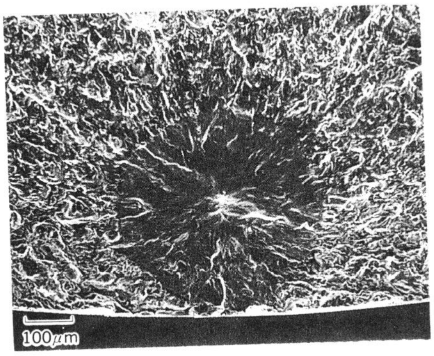

Figure 2 Example of fish-eye pattern on fracture surface fatigued at 400℃

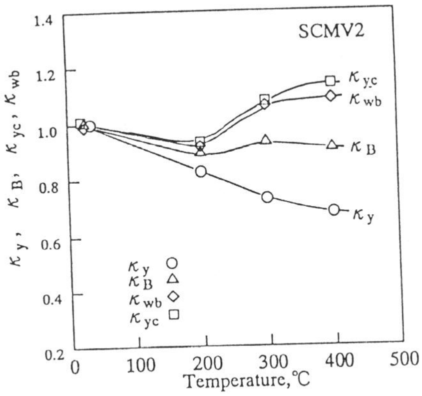

Figure 3 Temperature dependencies of deformation and strength properties

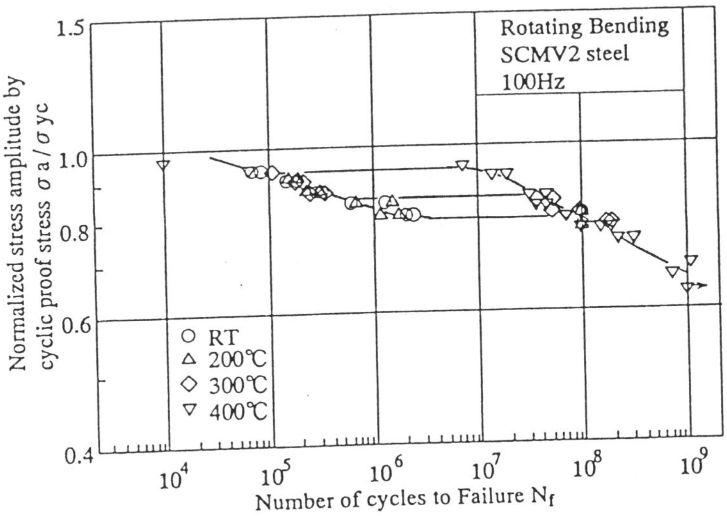

Figure 4 Rotating bending fatigue σ_a/σ_{yc}-N_f curves